Cell-Edge Detection via Selective Cooperation and Generalized Canonical Correlation

Mohamed Salah Ibrahim, *Student Member, IEEE*, Ahmed S. Zamzam, *Member, IEEE*, Aritra Konar, *Member, IEEE*, and Nicholas D. Sidiropoulos, *Fellow, IEEE*

Abstract-Improving the uplink quality of service for users located around the boundaries between cells is a key challenge in cellular systems. Existing approaches relying on power control throttle the rates of cell-center users, while multi-user detection requires accurate channel estimates for the cell-edge users, which is another challenge due to their low received signal-to-noise ratio (SNR). Utilizing the fact that cell-edge user signals are weak but common (received at roughly equal power) at different base stations (BSs), this paper establishes a connection between cell-edge user detection and generalized canonical correlation analysis (GCCA). It puts forth a GCCA-based method that leverages selective BS cooperation to recover the cell-edge user signal subspace even at low SNR. The cell-edge user signals can then be extracted from the resulting mixture via algebraic signal processing techniques. The paper includes theoretical analysis showing why GCCA recovers the correct subspace containing the cell-edge user signals under mild conditions. The proposed method can also identify the number of cell-edge users in the system, i.e., the common subspace dimension. Simulations reveal significant performance improvement relative to various multiuser detection techniques. Cell-edge detection performance is further studied as a function of how many / which BSs are selected, and it is shown that using the closest three BS is always the best choice.

Index Terms—Generalized canonical correlation analysis (GCCA), multi-user detection, cellular networks, cell-edge users, uplink detection, base station cooperation, identifiability, multiple-input-multiple-output (MIMO).

I. INTRODUCTION

PROVIDING high data rates to users located at the boundaries between cellular coverage areas constitutes a major concern in the current 4G system [1] and the emerging 5G networks [2]. Even with advanced technologies such as multiple-input-multiple-output (MIMO) and orthogonal frequency division multiplexing (OFDM) [3], [4] in place, nomadic users who are close to the cell edge are still prone to suffer from significant performance degradation [5], [6].

Owing to the fact that the received signal power exhibits an inverse relationship with the propagation distance, cell-edge user terminals experience high path-loss that eventually results in a severe performance degradation [7]. This effect becomes more pronounced when mobile systems operate at higher radio

Original manuscript submitted March 26, 2020; revised December 6, 2020; accepted May 16, 2021. This work was supported by the National Science Foundation (NSF) under Grant ECCS-1807660.

Mohamed Salah Ibrahim, Aritra Konar and Nicholas D. Sidiropoulos are with the Department of Electrical and Computer Engineering, University of Virginia, Charlottesville, VA, 22904 USA (e-mail: salah@virginia.edu; aritra@virginia.edu; nikos@virginia.edu).

Ahmed S. Zamzam is with the National Renewable Energy Laboratory, Golden, CO, 80401 USA (e-mail: ahmed.zamzam@nrel.gov)

frequency, as expected in the future [8], thereby rendering the cell-edge user detection problem even more difficult. A variety of techniques, ranging from multi-user detection [9], user scheduling [10], power control [11], cooperative communication [6], [12], and interference mitigation [13]–[15] have been proposed as possible candidates for tackling this problem.

Though optimal, the maximum likelihood detector (MLD) [9], [16] requires solving an NP-hard combinatorial problem with computational complexity that grows exponentially with the number of users, thereby precluding its use in practical multi-antenna systems. The so-called sphere decoder [17] (SD) is a near-optimal detector that can attain the MLD performance with lower complexity. However, it has been proven that its average complexity remains exponential [18]. In the low to moderate signal-to-noise ratio (SNR) regime, semi-definite relaxation (SDR) based methods [19], [20] can yield performance comparable to SD in polynomial time; yet their complexity remains unaffordable in terms of practical implementation at present [21].

Whereas equalization-based detectors such as zero-forcing (ZF) and minimum mean square error (MMSE) [22] exhibit substantially lower complexity compared to MLD, SD and SDR, their bit error rate (BER) performance often suffers severe degradation, especially at low SNR. The performance of both ZF and MMSE detectors can be further enhanced [23] by using successive interference cancellation (SIC), or decision feedback (DF) [24], [25], which rely on iteratively eliminating the strong (cell-center) user signals once they are decoded. While one can also resort to joint detection using base station cooperation [26], this often degrades the performance because of near-far effects and the inaccurate channel estimates of cell-edge users.

A major issue with all of the aforementioned detectors is that their performance is dependent on the availability of accurate channel state information of all users. This may be possible for users that are close to their serving base station (cell-center), and hence, reliable detection of such users can be guaranteed. On the other hand, owing to high path-loss, the signals of cell-edge (weak) users are received at low SNR, which degrades the quality of their channel estimates. This together with inter- and intra-cell interference have a deleterious impact on the BER performance of the cell-edge users [14].

Power control [11] and/or scheduling algorithms [10], [27] have proven to be successful in significantly improving the quality of service (QoS) of cell-edge users. This, however,

comes at the expense of throttling the cell-center user rates, and consequently the overall system throughput [11], [27], [28]. Moreover, the frequent mobility-induced hand-off of cell-edge users renders their detection task even more challenging [29].

The shortcomings of the prevailing approaches motivate the following question: Does there exist a low-complexity method that can provide reliable detection of the cell-edge users without knowing their channels or sacrificing the performance of cell-center users by resorting to power control and scheduling techniques?

This paper provides an affirmative answer to this question – by proposing an unsupervised learning-based method that leverages *selective* base station cooperation to recover celledge users signals at low SNR subject to strong inter- and intra- cell interference. Relying on fact that cell-edge users are located at approximately equal distances from different base stations, and hence their received signals are weak but *common* (meaning: they are received at low but roughly equal power at different base stations), this paper shows that reliable detection is possible via (generalized) canonical correlation analysis (G)CCA [30] under mild conditions.

While base station cooperation [31] has been considered before for several tasks such as coordinated power control [32], coordinated scheduling [33], and inter-cell interference mitigation [34], [35], cooperation here is utilized for a completely different purpose: as a means for cell-edge user detection, via GCCA. This work adds to the growing list of applications of (G)CCA in several areas in signal processing and wireless communications, ranging from array processing [36], direction-of-arrival (DoA) estimation [37], radar anti-jamming [38], blind source separation [39]–[42], speech processing [43], multi-view learning [43], [44], and more recently in cell-edge user detection using two BSs [45]. Efficient algorithms have been recently developed for handling large scale GCCA [46]–[48].

Our contributions in this paper are as follows:

• We extend our previous work [45], which proposed using classical two-view CCA to detect cell-edge user signals in a cellular network with two cells, to the more general setting. That is, we consider a scenario with L cells / views (L > 2) which involves GCCA [49], [50] as opposed to CCA for L=2. We propose a two-stage approach that uses cooperation to jointly detect cell-edge users signals without prior knowledge of their channel state information. In particular, we first consider the socalled MAXVAR formulation of GCCA [49], and show that it yields the range space of the cell-edge user signals. We present identifiability conditions under which the common subspace can be recovered. While identifiability conditions for the common subspace of two views have been obtained in [45], the conditions we provide here for the general case are more relaxed. Upon identifying the subspace comprising the cell-edge users signals via GCCA, we utilize the (R)ACMA [51] algorithm, which exploits the finite alphabet constraint of the user transmitted signals to retrieve the original cell-edge user signals from the resulting mixture. Fortunately, both MAXVAR

- GCCA and RACMA admit relatively simple algebraic solution via eigenvalue decomposition. This renders our approach computationally favorable in practice, because the proposed method for solving the cell-edge problem is tantamount to solving two eigenvalue decomposition problems.
- We present an elegant theoretical analysis which shows that GCCA can reliably estimate the common subspace in the presence of thermal noise and cross interference from users in adjacent cells, under realistic assumptions on the SNR of the different users.
- We provide an elegant GGCA strategy that can be used to classify users as cell-edge or cell-center, thereby determining the correct dimension of the common subspace.
- To showcase the effectiveness of our proposed method for cell-edge user detection, we provide a comprehensive suite of simulations that employs a realistic path-loss model from the 3GPP 38.901 standard. Experiments reveal that our approach attains a considerable improvement in the BER at low SNR under realistic levels of inter-cell interference and dense scenarios with a large number of cell-center users. We compare our proposed method with our previous CCA-based one and different multi-user detection techniques including ZF-SIC and MMSE-SIC which assume perfect knowledge of the cell-center user channels. We show that the proposed GCCA method achieves significant reduction in the BER compared to all baselines. Moreover, our simulations show that using GCCA with the three closest BSs always yields the best detection performance for the cell-edge users. That is, not only does using the three closest BSs always improves the results of using the two closest BSs; but also that using more than the three closest BSs never helps – neither of which was obvious a priori.

A. Paper Organization

The outline of this paper is as follows. After briefly reviewing (G)CCA in Section II, Section III defines the problem statement and highlights the major limitations of the prior cell-edge user detection methods. The proposed detector and the main results are presented in Section IV. Then, numerical simulations are provided in Section V. Conclusions are drawn in Section VI. Long proofs and derivations are relegated to the Appendix.

B. Notation

In this work, we use upper and lower case bold letters to denote matrices and column vectors, respectively. For any general matrix \mathbf{N} , we use \mathbf{N}^T , \mathbf{N}^H , \mathbf{N}^{-1} , \mathbf{N}^\dagger and $\mathrm{Tr}(\mathbf{N})$ to denote the transpose, the conjugate-transpose, the inverse (when it exists), the pseudo-inverse, and the trace of \mathbf{N} , respectively. $\mathbf{N}(:,m)$ denotes the m-th column of \mathbf{N} (MATLAB notation). Furthermore, $\mathrm{Re}\{\mathbf{N}\}$ and $\mathrm{Im}\{\mathbf{N}\}$ extract the real part and the imaginary part of \mathbf{N} , respectively. Scalars are represented in the normal face, while calligraphic letters are used to denote sets. $\|.\|_2$ and $\|.\|_F$ denote the ℓ_2 -norm and the Frobenius norm, respectively. Finally, \mathbf{I}_N and $\mathbf{0}_{N\times M}$

denote the $N \times N$ identity matrix and the $N \times M$ zero matrix, respectively.

II. PRELIMINARIES

Consider L data sets $\{\mathbf{Y}_\ell \in \mathbb{C}^{M_\ell \times N}\}_{\ell=1}^L$, where $\mathbf{y}_\ell^{(n)} := \mathbf{Y}_\ell(:,n)$ is an M_ℓ -dimensional feature vector that defines the ℓ -th view of the *n*-th sample, $\forall n \in \mathcal{N} := \{1, \dots, N\}$ and $\forall \ell \in \mathcal{L} := \{1, \cdots, L\}$. Without loss of generality, assume that all per-view data vectors $\{\mathbf{y}_{\ell}^{(n)}\}_{n=1}^{N}$ are zero-mean, otherwise the sample mean can be subtracted as a pre-processing step. While single-view analysis techniques, i.e., L = 1, like principal component analysis [52] aim at extracting strong components from the given data matrix, multi-view analysis tools such as coupled matrix factorization (CMF) or canonical correlation analysis (CCA), seek to jointly analyze different views of the data. The main difference between CMF and (G)CCA lies in the optimization criterion: whereas CMF uses a data fitting (usually: least squares) criterion, (G)CCA is based on a "differential" criterion that forces it to zoom in only on what is common between the different views. If one of the views includes a very strong component that is absent from the other view(s), a least squares CMF formulation can still be obliged to represent that component. (G)CCA, on the other hand, owing to its use of a differential (balancing) criterion, can ignore principal components no matter how strong they are, as long as they are not common. For instance, the two-view CCA, i.e., L=2, looks for two lowdimensional subspaces $\mathbf{Q}_1 \in \mathbb{C}^{M_1 \times K_c}$ and $\mathbf{Q}_2 \in \mathbb{C}^{M_2 \times K_c}$ with $K_c \ll \min\{N, M_\ell\}$, such that the distance between the linear projections of the received signals Y_1 and Y_2 onto these subspaces is minimized. From an optimization perspective, the distance-minimization formulation of the twoview CCA can be expressed as [53]

$$\begin{aligned} & \min_{\mathbf{Q}_1, \mathbf{Q}_2} \ \|\mathbf{Y}_1^H \mathbf{Q}_1 - \mathbf{Y}_2^H \mathbf{Q}_2\|_F^2 \\ & \text{s.t.} \quad \mathbf{Q}_\ell^H \mathbf{Y}_\ell \mathbf{Y}_\ell^H \mathbf{Q}_\ell = \mathbf{I}, \ \forall \ \ell = \{1, 2\} \end{aligned} \tag{1a}$$

s.t.
$$\mathbf{Q}_{\ell}^{H} \mathbf{Y}_{\ell} \mathbf{Y}_{\ell}^{H} \mathbf{Q}_{\ell} = \mathbf{I}, \ \forall \ \ell = \{1, 2\}$$
 (1b)

The columns of \mathbf{Q}_{ℓ} are called the canonical components of the ℓ -th view. Problem (1) can be optimally solved via generalized eigenvalue decomposition [40], [54]. To generalize problem (1) to consider the case of multiple views $(L \ge 3)$, it is natural to adopt a pair-wise matching criterion [49]. That is, we consider the optimization problem

$$\min_{\{\mathbf{Q}_{\ell}\}_{\ell=1}^{L}} \sum_{\ell=1}^{L-1} \sum_{\ell'>\ell}^{L} \|\mathbf{Y}_{\ell}^{H} \mathbf{Q}_{\ell} - \mathbf{Y}_{\ell'}^{H} \mathbf{Q}_{\ell'}\|_{F}^{2}$$
 (2a)

s.t.
$$\mathbf{Q}_{\ell}^{H} \mathbf{Y}_{\ell} \mathbf{Y}_{\ell}^{H} \mathbf{Q}_{\ell} = \mathbf{I}, \ \forall \ (\ell, \ell') \in \mathcal{L}.$$
 (2b)

Problem (2) is referred to as the sum-of-correlations (SUM-COR) generalized CCA [49]. Although SUMCOR is known to be NP-hard in its general form [55], [56], several efficient and scalable algorithms have been developed to obtain highquality approximate solutions [48], [55], [56].

Instead of minimizing the distance between the reduced-dimension views, another formulation seeks a low-dimensional common latent representation, namely

 $\mathbf{G} \in \mathbb{C}^{N imes K_c}$, of the different views. This leads to the socalled maximum-variance (MAXVAR) GCCA formulation, which is given by

$$\min_{\{\mathbf{Q}_{\ell}\}_{\ell=1}^{L},\mathbf{G}} \sum_{\ell=1}^{L} \|\mathbf{Y}_{\ell}^{H} \mathbf{Q}_{\ell} - \mathbf{G}\|_{F}^{2}$$
 (3a)

s.t.
$$\mathbf{G}^H \mathbf{G} = \mathbf{I}$$
. (3b)

Although both SUMCOR and MAXVAR aim at finding highly-correlated reduced-dimension views, and their solutions can be shown to coincide in the special case of L=2(CCA), they are generally different for L > 2 (GCCA). While problem (3) introduces an additional NK_c variables compared to SUMCOR, it replaces the multiple constraints in (2) with a single orthonormality constraint on the matrix G. Fortunately, the MAXVAR GCCA formulation admits algebraic solution via eigenvalue decomposition. To see this, one can fix G and solve (3) with respect to \mathbf{Q}_{ℓ} 's. Then, upon assuming that the matrices $\{\mathbf{Y}_\ell\}_{\ell=1}^L$ are full row rank, it follows that $\mathbf{Q}_{\ell}^{*} = (\mathbf{Y}_{\ell} \mathbf{Y}_{\ell}^{H})^{-1} \mathbf{Y}_{\ell} \mathbf{G}$. Substituting back \mathbf{Q}_{ℓ}^{*} in (3) and expanding the cost function in (3a), one can recast (3) as

$$\max_{\mathbf{G} \in \mathbb{C}^{N \times K_c}} \operatorname{Re} \{ \operatorname{Tr}(\mathbf{G}^H \mathbf{A} \mathbf{G}) \}$$
 (4a)

s.t.
$$\mathbf{G}^H \mathbf{G} = \mathbf{I}$$
. (4b)

where **A** is defined as $\mathbf{A} := \sum_{\ell=1}^{L} \mathbf{Y}_{\ell}^{H} (\mathbf{Y}_{\ell} \mathbf{Y}_{\ell}^{H})^{-1} \mathbf{Y}_{\ell}$. It can be easily seen that (4) is nothing but an eigenvalue problem with the optimal solution G^* being the first K_c principal eigenvectors of the matrix A [57].

In what follows, we will focus on the MAXVAR formulation to show how GCCA relates to the problem of cell-edge user detection in multi-cell, multi-user MIMO systems. Here, we adopted the MAXVAR formulation over the SUMCOR one as (i) it can be optimally solved using eigendecomposition whereas SUMCOR is an NP-Hard problem when the number of views (i.e., base stations in our context) exceeds two, (ii) is computationally cheaper compared to SUMCOR, and hence, it is practically preferable, and (iii) does not suffer from initialization and tuning parameters issues as SUMCOR does. Therefore, we see that considering MAXVAR will eventually lead to an overall much simpler approach that can solve the cell-edge detection problem.

III. SYSTEM MODEL

Consider an uplink transmission scenario in a cellular network with L regular hexagonal cells – each cell has a base station (BS) located at its center, as shown in Fig. 1. The ℓ -th BS is equipped with M_{ℓ} antennas, and serves K_{ℓ} single-antenna users. Let $K_{e_{\ell}}$ denote the number of celledge users served by the ℓ -th BS, with $K_{e_{\ell}} < K_{\ell}, \forall \ \ell \in$ $\mathcal{L} := \{1, \cdots, L\}$. The uplink channel vector representing the small-scale fading between the k-th user located in the j-th cell and the ℓ -th BS is given by $\mathbf{z}_{\ell kj} \in \mathbb{C}^{M_{\ell}}$. The entries of $\mathbf{z}_{\ell k i}$ are independent identically distributed (i.i.d.) complex Gaussian random variables with zero mean and variance $1/M_{\ell}$. This corresponds to a favorable propagation medium with rich scattering. The coefficient that accounts for

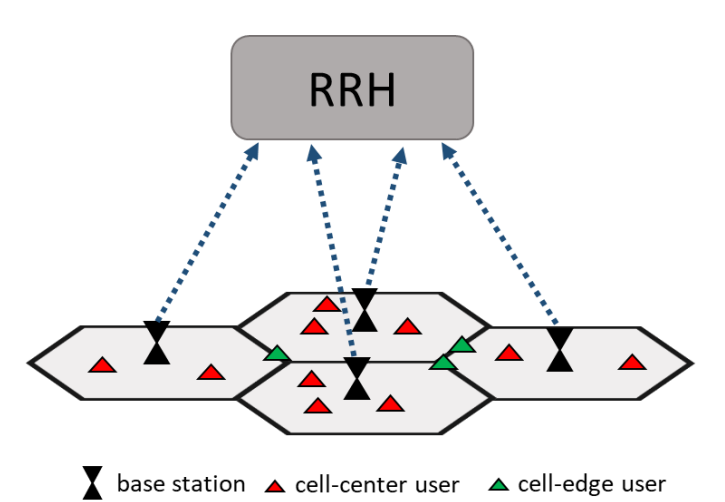


Fig. 1: System model

the signal attenuation due to distance (path-loss) between the ℓ -th BS and the k-th user in the j-th cell is given by $\alpha_{\ell kj} \in \mathbb{R}$. Accordingly, the overall uplink channel vector is given by

$$\mathbf{h}_{\ell kj} = \sqrt{\alpha_{\ell kj}} \mathbf{z}_{\ell kj},\tag{5}$$

Throughout this work, we assume that the channel vectors are *not* known a priori at the BSs.

A. Uplink Transmission

The considered users in the system are assumed to be allocated the same time-frequency resource. Also, assume that all user transmissions are heard at all BSs, thereby introducing both intra- and inter-cell interference at each BS. Also, all user transmissions are assumed to be synchronized at the BSs (this assumption can be lifted; see below and in [58]). Define $\mathbf{x}_{kj} \in \mathbb{C}^N$ as the vector transmitted by the k-th user in the j-th cell. The received signal, $\mathbf{Y}_\ell \in \mathbb{C}^{M_\ell \times N}$, at the ℓ -th BS is given by

$$\mathbf{Y}_{\ell} = \sum_{j=1}^{L} \sum_{k=1}^{K_j} \sqrt{p_{kj}} \mathbf{h}_{\ell k j} \mathbf{x}_{k j}^T + \mathbf{N}_{\ell}, \tag{6}$$

where $\mathbf{h}_{\ell kj}$ is the uplink channel response vector as defined in (5), p_{kj} is the transmitted signal power of the k-th user in the j-th cell. The term $\mathbf{N}_{\ell} \in \mathbb{C}^{M_{\ell} \times N}$ contains i.i.d. entries with zero mean and variance σ^2/N , i.e., $\mathbb{E}[\mathbf{N}_{\ell}\mathbf{N}_{\ell}^H] = \sigma^2\mathbf{I}$. Throughout this work, we assume that neither scheduling algorithms nor power control is employed. In other words, all users are always active, and all users are assigned the same transmission power, i.e., $p_{kj} = p, \forall k, j$. Scheduling and power control algorithms can still be employed on top of the proposed framework for additional traffic shaping and other system considerations.

In this paper, we assume that all BSs are connected to a remote radio head (RRH) via backhaul links which can be either microwave links or high speed optical fiber cables [31]. Each BS forwards its received signal to the RRH. Although base station cooperation has been considered in several earlier papers [32]–[35], it is adopted here for an entirely different

purpose. That is, we exploit the joint processing of the BS signals at the RRH to provide reliable detection of celledge users whose signals are received at low SNR without knowledge of any of the user channels. One key challenge for all the BS cooperation techniques in the literature is time synchronization [31] of the received signal at the RRH. Even though all prior works assumed perfect synchronization at the RRH [6], we recently developed a low-complexity CCA-based algorithm that can handle (lack of) synchronization for two BSs [58], and can be easily modified to deal with the multicell case.

B. Prior Art: Limitations and Challenges

We now provide a brief discussion of the limitations of the prior art used to detect cell-edge user signals. To this end, it is convenient to write (6) as

$$\mathbf{Y}_{\ell} = \mathbf{H}_{\ell p_{\ell}} \mathbf{X}_{p_{\ell}}^{T} + \mathbf{H}_{\ell e_{\ell}} \mathbf{X}_{e_{\ell}}^{T} + \sum_{j \neq \ell}^{L} \mathbf{H}_{\ell j} \mathbf{X}_{j}^{T} + \mathbf{N}_{\ell}, \quad (7)$$

where we collect the transmitted signals of the cell-center users and the cell-edge users served by the ℓ -th BS in the matrices $\mathbf{X}_{p_\ell} \in \mathbb{R}^{N \times (K_\ell - K_{e_\ell})}$ and $\mathbf{X}_{e_\ell} \in \mathbb{R}^{N \times K_{e_\ell}}$, respectively, and the transmitted signals by the users served by the j-th BS in $\mathbf{X}_j \in \mathbb{R}^{N \times K_j}$. Further, the matrices $\mathbf{H}_{\ell p_\ell} \in \mathbb{C}^{M_\ell \times (K_\ell - K_{e_\ell})}$, $\mathbf{H}_{\ell e_\ell} \in \mathbb{C}^{M_\ell \times K_{e_\ell}}$ and $\mathbf{H}_{\ell j} \in \mathbb{C}^{M_\ell \times K_j}$ hold on their columns the respective channel vectors. Note that we absorbed the transmitted signal power p of each user in its channel vectors.

The goal is to recover the cell-edge user signals, $X_{e_{\ell}}$, from the received signal \mathbf{Y}_{ℓ} . The traditional approach to recover $\mathbf{X}_{e_{\ell}}$ is to first estimate all user channels via transmitting orthogonal pilots, and then employ the ZF or MMSE detector to decode cell-edge user signals using their estimated channel. This approach usually fails to provide reasonable performance due to the effect of intra-cell interference (transmissions of strong cell-center users), the effect of inter-cell interference (transmissions from users in other cells) and noise. The signals of cell-edge users are consequently received at very low signal to interference plus noise ratio (SINR), which causes high uncertainty in their channel estimates, which in turn seriously degrades their detection performance. One workaround is to use ZF or MMSE followed by successive interference cancellation to decode and subtract the cell-center user signals, thereby mitigating / eliminating the intra-cell interference effect. While this approach can slightly improve the detection performance, the inter-cell interference and channel estimation errors still cause severe performance degradation.

Another potential solution that mitigates the inter-cell interference effect [59], and can indeed enhance the detection of such users, is to use power control and/or scheduling algorithms together with BS cooperation techniques [60]. However, this comes at the expense of throttling the transmission of cell center users, and hence, it also severely degrades the overall system throughput.

In the forthcoming section, we will present a two-stage learning-based approach that leverages BS cooperation to reliably identify cell-edge user signals without knowing their channels, and without resorting to either power control or scheduling.

IV. PROPOSED DETECTOR AND IDENTIFIABILITY ANALYSIS

The cell-edge users are located far but at roughly equal distances from different BSs. In other words, if we use the distance-power relationship, their received signals are weak but common to multiple BSs, i.e., their signals are received at relatively equal power at different BSs. We will show how GCCA can efficiently recover the cell-edge users' signal range space at low SNR, even if they are buried under strong intraand inter-cell interference. Notice that, owing to the broadcast nature of the wireless medium, all user transmissions are (over)heard, albeit weakly, at all BSs. Hence all user signals are, in principle, common. However, we use the phrases "common" for cell-edge users versus "private" for cell-center users to reflect the power (im)balance of different users. That is, cell-center users signals are received at very high SNR, e.g., [20, 30] dB, at their serving BS, and very low SNR, eg. [-10, -30] dB at non-serving BSs. On the other hand, celledge user signals are received at low but roughly equal SNR, e.g., [3, 5] dB at multiple BSs.

From the geometry of the hexagonal cells shown in Fig. 1, one can argue that a user can be common to two or three BSs, i.e., it can be located at relatively equal distance from two or three BSs. For example, a user located on the left corner of the common edge between the top and bottom cells in Fig. 1 is common to the BSs in these two cells and the one on the left. Based on this fact, we will design a detector that can recover cell-edge user transmitted signals from the signal received at three BSs. The case of more than three will also be considered in the simulations section.

Remark 1. It is worth pointing out that we have only considered the uniformally hexagonal cells architecture and the roughly-equidistant assumption of cell-edge users for the ease of exposition. We only need the relative delays of the different users to be the same at each of the L=3 BSs (so that the associated views contain the same cell-edge subspace) and the received SNRs for the cell-edge users to be at least a few dB above the noise floor. The latter typically holds even when shadowing is considered. Being approximately equidistant from the 3 BSs is one reasonable way to motivate these assumptions, but it is not the only one (e.g., small cells and per-subcarrier processing). Furthermore, while with shadowing coefficients the received SNR at the different views will not be balanced, our approach does not necessarily require the received SNR to be fully balanced at the different views, as we will see in the simulations.

We will first consider the noiseless case to find the identifiability conditions required to recover the cell-edge user signals. Identifiability is very important as it provides sufficient conditions under which the recovery of the cell-edge user signals via (G)CCA is guaranteed under ideal (noiseless) conditions. Whereas we have derived identifiability conditions in the case of two BSs [45], it turns out that the conditions for three

BSs are more relaxed (details will be provided in the next subsection).

A. Noiseless Case

Let $K_c = \sum_{j=1}^{L} K_{e_j}$ denote the total number of cell-edge users. Assume that all cell-edge users are located around the intersection point of the three hexagonal cells. Thus equation (7), with L = 3, can be rewritten as

$$\mathbf{Y}_{\ell} = \mathbf{H}_{\ell p_{\ell}} \mathbf{X}_{p_{\ell}}^{T} + \mathbf{H}_{\ell c} \mathbf{X}_{c}^{T} + \sum_{j \neq \ell}^{L} \mathbf{H}_{\ell p_{j}} \mathbf{X}_{p_{j}}^{T} + \mathbf{N}_{\ell}, \quad (8)$$

where the subscripts ' p_ℓ ' and 'c' stand for private to the ℓ -th BS and common to all base stations, respectively. The matrices $\mathbf{X}_c \in \mathbb{R}^{N \times Kc}$ and $\mathbf{X}_{p_j} \in \mathbb{R}^{N \times (K_j - K_{e_j})}$ hold the transmitted signals of the cell-edge users and cell-center users in the j-th cell, respectively. Accordingly, $\mathbf{H}_{\ell c} \in \mathbb{C}^{M_\ell \times K_c}$ and $\mathbf{H}_{\ell p_j} \in \mathbb{C}^{M_\ell \times (K_j - K_{e_j})}$ hold on their columns the corresponding channel vectors. Further, we define $\mathbf{E}_\ell := \sum_{j \neq \ell}^L \mathbf{H}_{\ell p_j} \mathbf{X}_{jp_j}^T + \mathbf{N}_\ell$ to denote the summation of intercell interference and noise at the ℓ -th BS. Thus, (8) can be rewritten as

$$\mathbf{Y}_{\ell} = \mathbf{H}_{\ell p_{\ell}} \mathbf{X}_{p_{\ell}}^{T} + \mathbf{H}_{\ell c} \mathbf{X}_{c}^{T} + \mathbf{E}_{\ell}, \tag{9}$$

Our goal now is to recover the cell-edge user signals \mathbf{X}_c given $\{\mathbf{Y}_\ell\}_{l=1}^L$. We will start by showing how the solution of the MAXVAR GCCA formulation (3) is related to the column space of the cell-edge user signals, and then we will explain how the original signals can be recovered from the given solution. Upon defining the matrix $\mathbf{V}^{(L)} \in$

$$\mathbb{C}^{(L-1)N\times((L-1)K_c+\sum\limits_{\ell=1}^L(K-K_{e_\ell}))} \text{ as follows,}$$

$$\mathbf{V}^{(L)} = egin{bmatrix} \mathbf{X}_{p1} & -\mathbf{X}_c & \mathbf{X}_{p2} \ dots & \ddots & \ddots & \ \mathbf{X}_{p1} & & -\mathbf{X}_c & \mathbf{X}_{pL} \end{bmatrix},$$

we have the following result.

Theorem 1. In the case where $\mathbf{E}_{\ell} = 0$, if the matrix $\mathbf{W}_{\ell} := [\mathbf{H}_{\ell c}, \mathbf{H}_{\ell p_{\ell}}] \in \mathbb{C}^{M_{\ell} \times (K_c + K_{\ell} - K_{e_{\ell}})}$ and the matrix $\mathbf{V}^{(L)} \in \mathbb{C}^{(L-1)N \times ((L-1)K_c + \sum\limits_{\ell=1}^{L} (K - K_{e_{\ell}}))}$ are full column rank, then the optimal solution \mathbf{G}^* of problem (3) is given by $\mathbf{G}^* = \mathbf{X}_c \mathbf{F}$, where \mathbf{F} is a $K_c \times K_c$ non-singular matrix.

Proof. See [61] which offers a comprehensive identifiability analysis of GCCA for general L.

Remark 2. The full column rank condition on \mathbf{W}_{ℓ} requires that: i) the number of antennas at each base station is greater than or equal to the number of users assigned to that base station, plus any cell-edge users associated with the other two base stations; and ii) the channel vectors of different users to be linearly independent. The first requirement is supported by massive MIMO technology that aims at equipping the base station with hundreds of antennas [62]. Further, because the user channel vectors can be assumed to be drawn from an absolutely continuous distribution (see (5)), the latter

condition is satisfied with probability one. The full column rank condition on V is related to the number of samples N required to guarantee recovery. For L=3, we need: i) the number of samples to be at least equal to the total number of cell-edge users plus one half the total number of cell-center users served by the three BSs; and ii) the transmitted sequences of different users to be linearly independent. For finite alphabets, the two conditions are satisfied with very high probability for modest N, as the user transmissions are statistically independent. In addition, it can be easily seen that the requirement on the number of samples N becomes less restrictive for L>2 compared to the earlier results for the two-view case in [45].

Theorem 1 asserts that in an ideal scenario where the effect of inter-cell interference and thermal noise is negligible compared to the intra-cell interference, GCCA successfully recovers the subspace spanned by the cell-edge users signals, under mild conditions. We point out that such a scenario can arise in practice, especially if all cell-center users are close to their serving BS. An interpretation of the statement of Theorem 1 is that if there exist several spatio-temporal signal views that contain very strong but different components (in our case here arising from the transmissions of each group of cell-center users) and very weak but common components (in our case here the received cell-edge user signals), then GCCA recovers the common components range space irrespective of the power of the individual components.

However, in practical deployment scenarios we cannot guarantee the above idealized assumptions. One of the main contributions of this paper is that it offers an analysis of GCCA performance in a realistic scenario with inter-cell interference and noise. This is coming up next.

B. Noisy Case

We now provide analysis showing how cell-edge users signals can be identified when $\mathbf{E}_\ell \neq 0$. In particular, we show that the signal subspace recovered by identifying the K_c principal eigenvectors of \mathbf{A} is indeed containing the cell-edge user transmitted messages. As shown earlier, this is equivalent to solving the MAXVAR GCCA problem.

Upon defining $K_s = \sum_{\ell=1}^{L} K_{\ell}$, let us write (8) in a more compact form as

$$\mathbf{Y}_{\ell} = \mathbf{H}_{\ell} \mathbf{X}^T + \mathbf{N}_{\ell},\tag{10}$$

where $\mathbf{H}_{\ell} = [\mathbf{H}_{\ell c}, \mathbf{H}_{\ell p_1}, \cdots, \mathbf{H}_{\ell p_L}] \in \mathbb{C}^{M_{\ell} \times K_s}$, and $\mathbf{X} = [\mathbf{X}_c, \mathbf{X}_{p_1}, \cdots, \mathbf{X}_{p_L}] \in \mathbb{C}^{N \times K_s}$. Further, we can use (5) to factor $\mathbf{H}_{\ell} = \mathbf{Z}_{\ell} \mathbf{P}_{\ell}^{1/2}$, where the columns of \mathbf{Z}_{ℓ} are the channel vectors representing small scale fading between the k-th user and the ℓ -th BS, for $k \in \mathcal{K}_s := \{1, \cdots, K_s\}$. Accordingly, each entry of the diagonal matrix \mathbf{P}_{ℓ} represents the corresponding received signal power that incorporates the transmitted power and the path-loss between each user and the ℓ -th BS. Thus, (10) can be equivalently written as

$$\mathbf{Y}_{\ell} = \mathbf{Z}_{\ell} \mathbf{P}_{\ell}^{1/2} \mathbf{X}^{T} + \mathbf{N}_{\ell}, \tag{11}$$

Assumption 1 (AS1). Assume that the matrices \mathbf{Z}_{ℓ} and $\mathbf{C} := \mathbf{X}/\sqrt{N}$ are approximately orthonormal, i.e., $\mathbf{Z}_{\ell}^H \mathbf{Z}_{\ell} \approx \mathbf{I}_{M_{\ell}}$ for all $\ell \in \mathcal{L}$ and $\mathbf{C}^H \mathbf{C} \approx \mathbf{I}_{K_s}$.

Remark 3. Recall that the matrices \mathbf{Z}_{ℓ} contain i.i.d entries with zero mean and variance $1/M_{\ell}$, and hence, the approximate orthonormality assumption on \mathbf{Z}_{ℓ} requires the number of base station antennas to be greater than the total number of users assigned to all base stations, and large enough for the sample average (inner product of different columns) to be close to the ensemble average (0). This requirement on the number of antennas is supported by massive MIMO technology that aims at equipping base stations with hundreds of antennas. On the other hand, the approximate orthonormality of \mathbf{C} requires the sequence length to be greater than the total number of users and the columns of \mathbf{C} to be linearly independent. For finite alphabets, the latter condition is satisfied with very high probability for modest N.

Let $\gamma_{k\ell}$ denote the received SNR of the k-th user at the ℓ -th BS. Then, we define $r_{k\ell}$ as

$$r_{k\ell} := \frac{\gamma_{k\ell}}{\gamma_{k\ell} + 1},$$

for all $k \in \mathcal{K}_s$ and $\ell \in \mathcal{L}$. For any user k, the multi-view correlation measure η_k is defined as $\eta_k := \sum_{\ell=1}^L r_{k\ell}$. We will make use of the following assumption on the cell-edge users.

Assumption 2 (AS2). For any cell-edge user i and cell-center user j, $\eta_i > \eta_j$.

Remark 4. Empirically, the relation between the average received power P_r and the distance is determined by the expression $P_r \propto d^{-\lambda}$ where d and λ denote the distance and the path loss exponent, respectively. The noise power at the receiver is given by σ^2 . Then, the value of $r_{k\ell}$ as function of the distance between the user and the BS $(d_{k\ell})$ is given by

$$r_{k\ell} = \frac{(d_{k\ell})^{-\lambda}}{(d_{k\ell})^{-\lambda} + \sigma^2/c},\tag{12}$$

where c is constant that depends on the communication medium and the antenna characteristics. This function exhibits a sharp phase transition which means that the ratio $r_{j\ell}$ for cell-center users at other cells is almost zero if they are dropped up to certain distance from their serving BS such that their received SNR at their non-serving BSs is a few dBs below zero, while all the ratios $r_{i\ell}$ for cell-edge users at their adjacent BSs is close to one if their received SNR at those BSs is a few dBs above zero.

Our main result is the following:

Proposition 1. In the presence of inter-cell interference and additive noise, under assumptions (ASI) and (AS2), the optimal solution \mathbf{G}^* of problem (3) is given by $\mathbf{G}^* \cong \mathbf{X}_c \mathbf{P}$ where \mathbf{P} is any $K_c \times K_c$ non-singular matrix.

Proof. The proof is relegated to the Appendix. \Box

We have thus showed that MAXVAR GCCA identifies the range space of the cell-edge users signals, under realistic

conditions. We will next show how the original signals \mathbf{X}_c can be unraveled from their range space, by exploiting their constellation/modulation structure.

C. ACMA Stage

Given the subspace G^* , the problem of recovering the user signals X_c can then be posed as

$$\min_{\mathbf{X}_c, \mathbf{F}} \|\mathbf{G}^* - \mathbf{X}_c \mathbf{F}\|_F^2 \tag{13a}$$

s.t.
$$\mathbf{X}_c(i,j) \in \Omega$$
, (13b)

where $\mathbf{X}_c(i,j)$ represents the (i,j)-th entry of the matrix \mathbf{X}_c , for $i=1,\cdots,N$ and $j=1,\cdots,K_s$. Although problem (13) is known to be NP-Hard even if \mathbf{F} is known, the Analytical Constant Modulus Algorithm (ACMA) developed by van der Veen [63] provides a good algebraic solution which comes with certain identifiability guarantees. In particular, ACMA transforms (13) to a generalized eigenvalue problem. While the obtained solution is subject to both phase and permutation ambiguities, both of them can be resolved in practice by simply matching the preamble of each estimated signal with the identification sequence that is known *a priori* at the serving BS.

It is worth emphasizing that the proposed end-to-end detector of the cell-edge user signals only requires solving two generalized eigenvalue problems. Therefore, the overall computational complexity of our proposed method is dominated by the complexity of solving two generalized eigenvalue problems. This renders our approach favorable for practical implementation.

We also point out that our proposed method works for any modulation scheme and even for analog signals. It is obvious that GCCA (first stage) can identify the common subspace irrespective of the modulation of the cell-edge user signals. The second stage exploits knowledge of the modulation to unravel the constituent signals from their range space. ACMA [63], for instance, deals with constant modulus communication signals such as higher-order PSK, QPSK or even analog phase or frequency-modulated signals. For binary signals (BPSK), the so-called real ACMA (RACMA) [51] can be used to recover the user signals. Furthermore, algorithms such as SIC-ILS [64] or the approach in [61] can be utilized for higher-order QAM – SIC-ILS can also exploit Forward Error Control (FEC) codes to further improve the decoding accuracy.

Throughout this work, we assume that the cell-edge users employ BPSK, QPSK, and 8PSK modulation, and hence, as we will see in the simulations, we use either RACMA [51] to recover the BPSK signals or ACMA [63] for QPSK and 8PSK modulation. Recall that the received signals of the cell-edge users are naturally weak, hence these users will typically employ low-order modulation.

D. Choosing the common subspace dimension

Recall that in our analysis in the Appendix, in order to differentiate between cell-center users and cell-edge users, we assumed that cell-center users are dropped up to certain distance from their serving BS (see Remark 3). However, if

all users are randomly dropped throughout the cells, then it is not obvious how to differentiate if a user has to be treated as a cell-center or a cell-edge user. In other words, how to determine the common subspace dimension if the cell-center users are fully scattered within their cell. Note that underestimating the common subspace dimension can naturally lead to a performance degradation as we will see in the simulation section. To overcome such an issue, we propose a GCCA-based algorithm that can accurately estimate the number of cell-edge users (common subspace dimension), and hence, we can classify whether a user is cell-center or cell-edge.

Exploiting the fact that a component that is common to three views should also be common to each pair of the three views, the common subspace dimension can be accurately estimated via checking the mean of correlation coefficients computed from the canonical components of each pair. Recall that $K_c \leq \min\{2M_\ell, N\}$, where K_c is the number of canonical pairs that can be extracted using GCCA. Upon solving problem (3) and obtaining the solutions $\{\mathbf{Q}_\ell^\star\}_{\ell=1}^3$, we define the i-th correlation coefficient between views j and ℓ as [61],

$$\rho_{\ell j}^{(i)} = \operatorname{Re}\{\mathbf{Q}_{\ell}^{H}(:,i)\mathbf{Y}_{\ell}\mathbf{Y}_{j}^{H}\mathbf{Q}_{j}(:,i)\}$$
(14)

 $\forall \ell, j \in \mathcal{L}$ and $j > \ell$ and $i \in \{1, \cdots, K_c\}$. Afterwards, we compute the i-th average correlation coefficient as $\rho_{\text{avg}}^{(i)} = \frac{1}{3}(\rho_{12}^{(i)} + \rho_{13}^{(i)} + \rho_{23}^{(i)})$, Then, we decide that the i-th canonical components $(\mathbf{Q}_1(:,i),\mathbf{Q}_2(:,i),\mathbf{Q}_3(:,i))$ extract a common signal if $\rho_{\text{avg}}^{(i)}$ is greater than a certain threshold – a reasonable choice of ρ_{th} is 0.5.

It is worth emphasizing that the proposed GCCA approach requires solving a generalized eigenvalue problem which naturally yields $\min\{M_\ell, T\}$ canonical vectors. Once these vectors are obtained, we use our proposed method to estimate the exact number of relevant canonical vectors, i.e., number of cell-edge users K_c , which will be later used to recover the common subspace from the data matrices $\{\mathbf{Y}_\ell\}_{\ell=1}^3$.

V. EXPERIMENTAL RESULTS

In this section, we use realistic numerical simulations to assess the performance of the proposed GCCA approach. We consider a scenario with L=4 hexagonal cells, each of radius R = 600 meters. The locations of cell-center users served by each BS are drawn uniformly at random within a distance less than d = 0.4R from their serving BS, unless stated otherwise. Cell-edge users, on the other hand, are located around the edges between base stations at distance between 0.95R and 1.05R. Fig. 2 shows one simulated scenario where cell-center users and cell-edge users are colored in red and green triangles, respectively. The transmitted power of all users was set to 25 dBm while the transmitted sequence length N was fixed to 800. We assume BPSK modulation for all the users, unless stated otherwise. All results were averaged over 500 Monte Carlo trials. Additive white Gaussian noise was used with variance σ^2 so that the SNR is P_e/σ^2 , where P_e is the average received power of cell-edge users. In fact, this enables us to evaluate SNR values required for cell-edge users

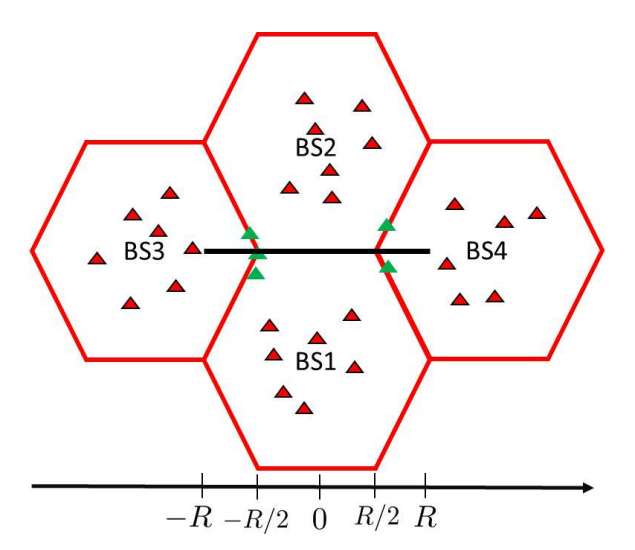


Fig. 2: Snapshot from the simulated scenario.

to achieve a specific BER. The uplink channel between the k-th user in the j-th cell and the ℓ -th BS is modeled as

$$\mathbf{h}_{\ell k j}^{H} = \sqrt{\frac{1}{M}} \sum_{n=1}^{N_{p}} \sqrt{\alpha_{\ell k j}^{(n)}} \mathbf{a}_{r}(\phi_{k}^{(n)})^{H},$$
 (15)

where N_p is the number of paths between the ℓ -th BS and the k-th user in cell j, $\forall \{\ell,j\} \in \mathcal{L}$ and $k \in [K_s]$. To compute the path gain, $\alpha_{\ell k j}^{(n)}$, we use the path-loss model of the urban macro (UMa) scenario from Table 7.4.1-1 in the 3GPP 38.901 standard, with the carrier frequency set to 2 GHz, $\forall n, \ell, j, k$. Furthermore, all cell-center users are allowed to possibly have a line of sight (LOS) component to their serving BS according to the LOS probability expression for the UMa scenario in Table 7.4.2-1 in the 3GPP 38.901 standard; however, all cell-edge users have only non-LOS components. The term $\mathbf{a}_r(.)$ is the array response vector at the BS, and $\phi_k^{(n)} \sim \mathcal{U}[-\pi,\pi]$ denotes the azimuth angle of arrival of the n-th path associated with the k-th user. Assuming the BS is equipped with a uniform linear array with omni-directional antenna elements stretched over the vertical direction, then

$$\mathbf{a}_r(\phi) = [1, e^{ikd\cos(\phi)}, \cdots, e^{ikd(M-1)\cos(\phi)}]^T, \tag{16}$$

where $i = \sqrt{-1}$, $k = 2\pi/\lambda$, λ is the carrier wavelength and $d = \lambda/2$ is the spacing between antenna elements.

To assess the efficacy of our approach, we implement the following approaches and use them as performance baselines.

- MMSE / ZF with channel estimation: the channels of all users are estimated via transmitting sequences of orthogonal pilots with length of 250 each. Then, both the MMSE and ZF detectors are employed to decode the cell-edge user signals using their estimated channels.
- MMSE / ZF SIC (R)ACMA with channel estimation: the channels of the cell-center users associated with each BS are estimated first. Then, we use both the ZF-SIC and MMSE-SIC detectors to decode, and then subtract the reencoded signals of the cell-center users at their serving BS. Afterwards, we apply (R)ACMA [51], [63] on the residual signal to recover the cell-edge user signals. To

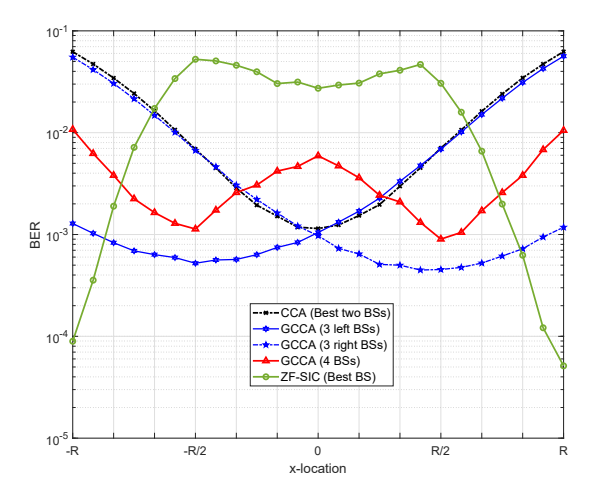


Fig. 3: BER vs. cell-edge user location: GCCA using 3 closest BSs is always better.

- guarantee fairness, since we assume BS cooperation, we feed (R)ACMA with the residual signals from all BSs simultaneously.
- MMSE / ZF SIC (R)ACMA Perfect: similar to the previous baseline but with perfect knowledge of the cellcenter user channels at their serving BS.
- CCA (R)ACMA combined: we use CCA to recover the range space of the cell-edge users from the nearest two BSs [45]. Then, we apply (R)ACMA to recover the cell-edge user signals from the resulting subspace.

In the first experiment, we consider a setup with $M_{\ell} = 12$ antennas and $K_{\ell} = 8$ single transmit antenna users, $\forall \ \ell \in$ \mathcal{L} . Considering the scenario shown in Fig. 2, we varied the x-location of one cell-edge user on the black edge between BS1 and BS2 from x = -R to x = R, while the locations of all other users are kept fixed during the experiment. At each value of x, we report the BER of the proposed GCCA approach using the three closest BSs, GCCA using all BSs, CCA using the closest two BSs and ZF-SIC RACMA with perfect cell-center users channels using the best BS. Note that when the user is located at x = -R/2, its received SNR is approximately equal to 3dB at BSs 1,2 and 3, according to our adopted path-loss model. As the user's location shifts towards the center (x = 0) of the black edge, its received SNR increases (as path-loss decreases) at BSs 1, 2, and 4 while it decreases at BS 3. When this user passes the center of the edge, the received SNR decreases again at BSs 1 and 2. On the other hand, when the user's location changes towards the very left corner of the black edge (x = -R), its received SNR automatically increases at BS 3, while it decreases at BSs 1, 2, 4.

As Fig. 3 depicts, when the user is located at x = -R/2 (the user is at relatively equal distance from three BSs), the proposed GCCA using the three left BSs (1, 2, and 3) attains the minimum BER compared to GCCA using all BSs, CCA using the two closest BSs and ZF-SIC using the best BS. Similarly, when the user is located at x = R/2, the

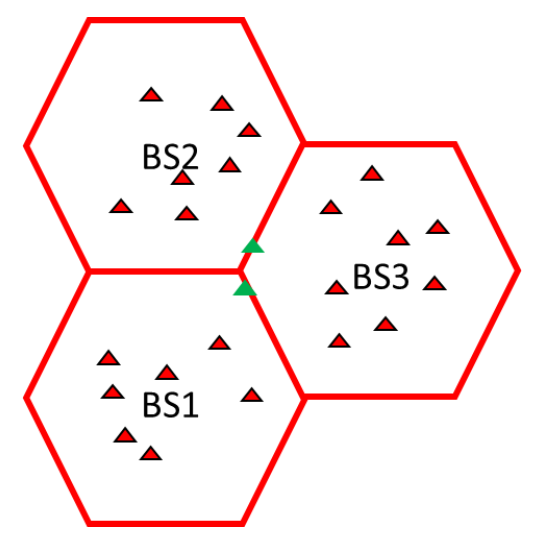


Fig. 4: Snapshot from the three BSs simulated scenario.

joint detection using the three BSs 1, 2, and 4 gives the best performance. When the user is close to $x=\pm R/2$, GCCA using the three nearest BSs attains more than order of magnitude reduction in the BER relative to CCA RACMA and much more relative to ZF-SIC RACMA.

On the other hand, as the location of the user moves towards the center of the cell-edge (x=0), the detection performance of CCA using the two BSs 1, 2 improves gradually until it reaches its best at the origin (minimum path-loss and maximum received SNR), and then it decreases again as shown in Fig. 3. This happens as the received SNR of the user's signal at BS 1 and BS 2 becomes higher, and considerable discrepancy becomes evident between the received SNR at BSs 1 and 2 and at BS 3. Note that GCCA using the best three BSs always yields the minimum BER when the user's location is in the interval [-R/2, R/2].

When the cell-edge user location becomes close to either BS 3 or BS 4, i.e., $x \approx \pm R$, Fig. 3 shows that using ZF-SIC RACMA at the nearest BS achieves the best detection performance among all other methods that use joint detection. This can be attributed to the fact that this user is no longer a "common" user - there is a large discrepancy among the received SNR at BS 3 (very high) and at BSs 1, 2, and 4 (very low), and hence, the power imbalance severely affects the detection performance of the (G)CCA based approaches. This observation suggests that depending on the user's type (center or edge), one should use either the closest BS or the three nearest BSs to detect the user. In other words, if a user is relatively close to any BS, then this user's signal received power is high at this BS and very weak at all other BSs, and hence, it makes sense to decode this user's signal from the nearest BS. However, if a user is close to the edge between cells, then this user is common to multiple BSs and jointly detecting such a user from the three closest BSs using GCCA yields the best detection performance.

More interestingly, it turns out that adding more BSs does not always improve the performance. For instance, at $x = \pm R/2$, while GCCA using four BSs attains a comparable

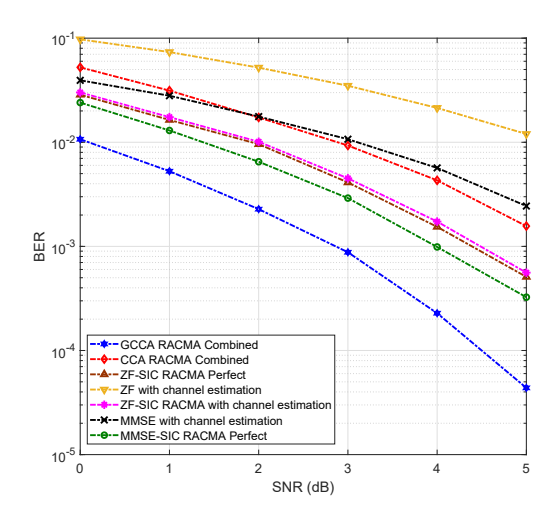


Fig. 5: BER vs. SNR of cell-edge users.

performance relative to GCCA with the three nearest BSs, the latter is considerably better as the user moves towards the center x = 0. This is because at x = 0, the received SNR is very low at both BS 3 and BS 4 compared to BS 1 and BS 2, and consequently, both views 3 and 4 act as two "noisy" views that naturally degrade the signal recovery of the cell-edge user. Therefore, one can conclude that from the geometry of the hexagonal cells, adding more BSs and feeding their received signals to GCCA to recover the common subspace will further degrade the detection performance of cell-edge users as any additional BS (view) will lead to an additional noisy view that severely affects the cell-edge user's signal recovery. In other words, the more views (L > 3) GCCA uses, the more difficult it becomes to reveal common information from all views simultaneously. Therefore, using the observation that using GCCA with the three closest BSs always yields the minimum BER for cell-edge users, and to further show the effectiveness of our approach under different settings, we will only consider the three BSs scenario, shown in Fig. 4, for all subsequent experiments.

We now consider another experiment where we vary the transmitted power of the two cell-edge users from 20 dBm to 25 dBm which corresponds to approximately 0 dB to 5 dB SNR according to the adopted path-loss model, while the transmitted power of all-center users is fixed to 25 dBm. Drawing different cell-center user locations for each Monte-Carlo realization, we compute the average BER among the two cell-edge users as a function of their transmitted power. Fig. 5 shows how GCCA provides significant improvement in the BER compared to all other methods. In particular, GCCA achieves an order of magnitude reduction in the BER compared to MMSE-SIC followed by RACMA (the second best method) which jointly detects the cell-edge user signals using the residual signals from the three BSs. Notice that, MMSE-SIC assumes perfect 'oracle' knowledge of the channels of cell-center users at their serving BS. This assumption becomes less realistic when "cell-center" users are fully scattered throughout the cell. Although this gives a big advantage to

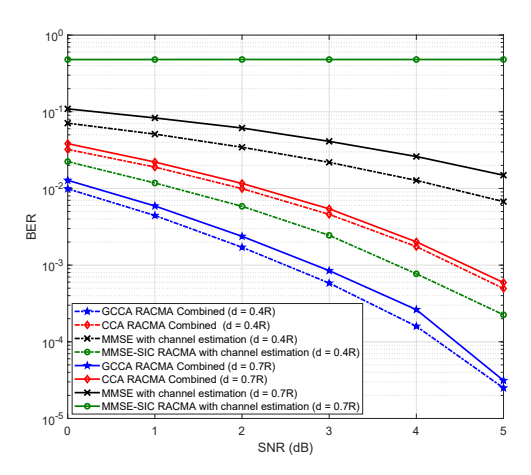


Fig. 6: BER vs. SNR of cell-edge users, d denotes the distance at which cell-center users are randomly dropped up to.

the MMSE-SIC approach, GCCA still provides considerably better detection performance of cell-edge users. Furthermore, one can easily see how the channel estimation errors severely degrade the detection performance of cell-edge users.

Additionally, we simulate a more realistic scenario where cell-center users are almost fully scattered in their cell. In particular, cell-center users are dropped up to d = 0.7R from their serving BS, thereby cell-edge users are experiencing more aggressive inter-cell interference compared to the case where d = 0.4R. Note that the MMSE-SIC RACMA is implemented using estimates of the cell-center users' channels instead of assuming perfect knowledge of their channels because that is hard to attain even approximately when cellcenter users are fully scattered. Fig. 6 depicts the inter-cell interference effect on the detection performance achieved by different methods. It is obvious that the MMSE-SIC RACMA completely fails at d = 0.7R compared to d = 0.4R. On the other hand, both GCCA and CCA have a slight degradation in their performance, which in turn reflects the efficacy of both methods that principally rely on recovering the subspace of the "equipowered" users. Note that GCCA with three BSs still attains an outstanding detection performance compared to the other methods under this realistic scenario.

We carry out another experiment in a more dense scenario where $K_\ell=16$ and $M_\ell=30$. Further, cell-center users are dropped up to d=0.8R. We report the BER of cell-edge users versus the SNR. Although the results in Fig. 7 show that the detection performance of all methods significantly degrades compared to the one in the previous experiment where $K_\ell=8$, our proposed approach still can attain acceptable performance by achieving 1e-3 BER at 5dB. Notice that doubling the number of users and allowing them to be more scattered naturally leads to greater corruption in the estimated common subspace, and hence, the degradation in the detection performance obtained by the proposed method is expected.

Adding more BSs with K users each might be expected to severely affect the performance which is true in general.

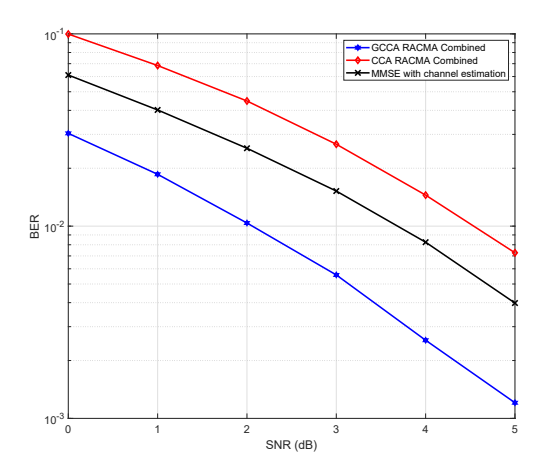


Fig. 7: BER vs. SNR of cell-edge users for different number of users.

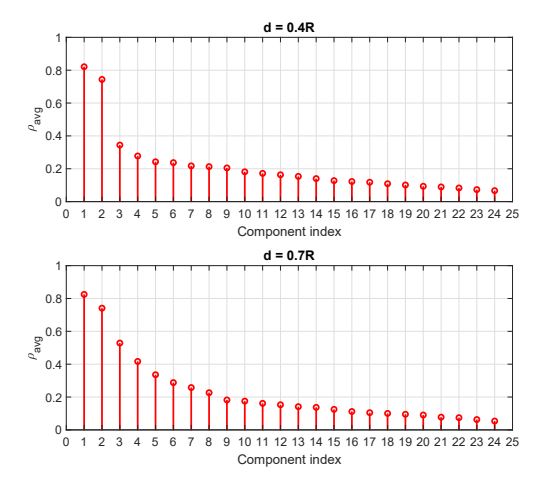


Fig. 8: Average correlation coefficient of all possible extracted components via GCCA.

However since, in principle, our approach recovers the subspace containing the "equipowered" user signals, adding more users in the far cells (not served by the three closest BSs) can slightly affect the cell-edge detection performance as we observed from our simulations. For instance, looking at Fig. 2, increasing the number of users served by BS 4 does not affect the BER obtained when the cell-edge user is located at x = -R/2 if GCCA is used with BSs 1, 2 and 3. However, increasing the number of cell-center users can only degrade the performance, as shown in Fig. 7, when these users are served by any of the BSs used for detecting the cell-edge users via GCCA. This can be attributed to the fact that there is a chance that some users could be included in the common part, and hence, underestimating the dimension of the common subspace can degrade performance.

We now test the proposed algorithm used to detect the number of cell edge users (i.e., the common subspace dimension). We consider a setup with $M_\ell=12,~K_\ell=8$, and SNR ≈ 3 dB. Note that since $2M_\ell < N$, we can find up to $2M_\ell$ canonical components. Fig. 8 shows the

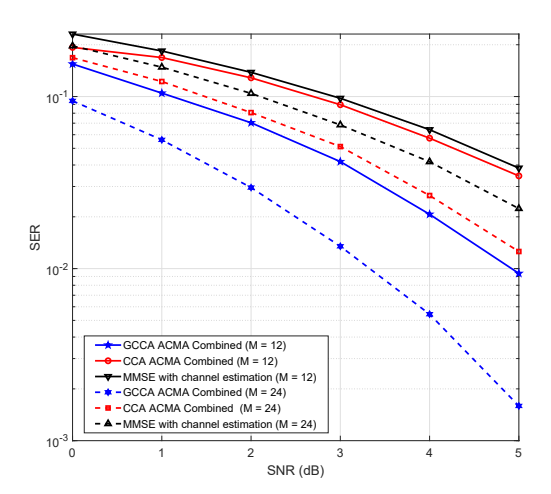


Fig. 9: SER vs. SNR of cell-edge users with QPSK modulation.

average correlation coefficient computed at the i-th extracted component, for $i = 1, \dots, 24$, for two different drop/scatter patterns for the cell-center users. It is obvious that when d = 0.4R, there is a significant gap between the average correlation coefficient of the first two components and the rest of the components. In particular, the average correlation coefficient of the first two components is almost 0.8 while all the rest are less than 0.3. Thus, one can decide that there exist only two cell-edge users in this case. On the other hand, at d = 0.7R, the value of the average correlation coefficient slightly increases for some of the components. For example, the average correlation coefficient of the third component now jumps to 0.52 which means that there is one more user that can be considered as common user. However, considering only the first two components is enough to reliably recover the signals of the two cell-edge users as shown in Fig. 6, where the detection performance was sightly affected by increasing d from 0.4R to 0.7R.

Finally, we evaluate the performance of the proposed method under different modulation schemes. First, we assume a QPSK transmission for all users in a scenario with $K_\ell=8$ users and two cell-edge users ($K_c=2$). Further, cell-center users are randomly located up to 0.7R from their serving BS. We report the symbol error rate (SER) vs SNR of cell-edge users for $M_\ell=M=12,24$ antennas, $\forall \ell$. As Fig. 9 depicts, GCCA followed by ACMA attains the lowest SER compared to both MMSE with channel estimation and CCA with the two closest BSs. It is also clear that, with M=12, the detection performance of all methods is worse for QPSK relative to BPSK in Fig. 6, as expected. However, as we double the number of antennas to M=24, a significant improvement can be achieved by our method, which attains approximately 10^{-3} SER at 5 dB SNR.

We also carried out another simulation with the previous setup but with 8PSK modulation instead of QPSK, and with $K_c=1$. The numerical results in Fig. 10 demonstrate the efficacy of our approach with higher-order modulation, in the low SNR region. Note that the detection performance of all

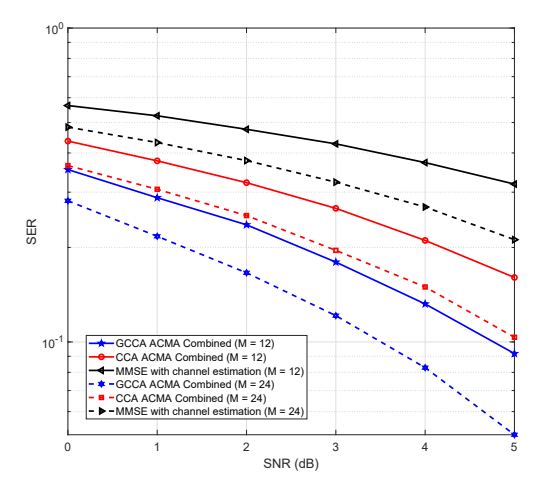


Fig. 10: SER vs. SNR of cell-edge users with 8PSK modulation.

methods degrades significantly as we increase the modulation order, which is expected given the SNR range considered. However, for higher order modulation, coding schemes can be employed on top of our proposed approach for improved reliability.

VI. CONCLUSIONS

We studied the problem of cell-edge user signal detection in the uplink of a multi-cell, multi-user MIMO system, with the aim of designing a detector that can reliably demodulate cell-edge user signals in the presence of strong intra-cell interference from cell-center users, without resorting to power control or/and scheduling algorithms that throttle the cellcenter user rates. We proposed a GCCA-based approach that leverages selective base station cooperation to reliably identify the common subspace containing cell-edge user signals at low SNR, without even knowing their channels. Then, we used an efficient analytical method ((R)ACMA) that guarantees the identifiability of finite alphabet signals from well-conditioned mixtures to separate the cell-edge user signals from the resulting subspace. The proposed method is appealing for use in dynamic environments because it (i) does not require any knowledge of the channel state information of cell-edge users; (ii) can automatically detect the number of common (celledge) user signals regardless of associated channel variations from one coherence interval to the next; (iii) can automatically adjust to varying PSK modulation order (so cell-edge users can even vary their modulation, depending on channel conditions); and (iv) can efficiently deal with synchronization issues.

We presented theoretical results to prove that under an idealized scenario, the proposed GCCA-based approach recovers the subspace containing the cell-edge user signals. Furthermore, we showed through an elegant analysis that under realistic assumptions on the inter-cell interference and the SNR of the cell-edge users, the common subspace recovery is guaranteed via GCCA. Simulations using a *realistic*

propagation and system model were carried out to show the superiority of the proposed learning-based method over the prevailing state-of-the-art methods. In particular, our proposed approach attained an order of magnitude reduction in the BER compared to other multi-user detection methods that assume perfect knowledge of the channels of the cell-center users. Furthermore, our experimental results evaluated the cell-edge user detection performance as a function of the number of cooperating BSs, and revealed that using the three closest BSs is always optimal in this regard. This was not obvious a priori, as intuition may have suggested that two or even more than three BSs might be preferable in certain cases.

APPENDIX A **PROOF OF PROPOSITION 1**

In this section, we will show that the principal K_c eigenvectors of the matrix

 $\mathbf{A} = \sum_{\ell=1}^{L} \mathbf{Y}_{\ell}^{H} (\mathbf{Y}_{\ell} \mathbf{Y}_{\ell}^{H})^{-1} \mathbf{Y}_{\ell}$ is approximately the column space of the cell-edge user signals. We first write the autocorrelation matrix $\mathbf{Y}_{\ell}\mathbf{Y}_{\ell}^{H}$ as

$$\mathbf{Y}_{\ell}\mathbf{Y}_{\ell}^{H} = \mathbf{Z}_{\ell}\mathbf{P}_{\ell}\mathbf{Z}_{\ell}^{H} + \sigma^{2}\mathbf{I},\tag{17}$$

where we have exploited the facts that, at $N > K_s$, $\mathbf{X}^T\mathbf{X}/N \approx \mathbf{I}_{K_s}$ and $\mathbb{E}[\mathbf{N}_\ell\mathbf{N}_\ell^H] = \sigma^2\mathbf{I}_{N_\ell}$. Define the diagonal matrix $\mathbf{\Gamma}_\ell := \mathbf{P}_\ell/\sigma^2 \in \mathbb{R}^{K_s \times K_s}$ that contains the received SNR of each user at the ℓ -th BS, and $\mathbf{U}_{\ell} := \mathbf{N}_{\ell}^H/\sigma \in$ $\mathbb{C}^{N\times M_\ell}$, and the matrix $\mathbf{A}_\ell := \mathbf{Y}_\ell^H(\mathbf{Y}_\ell\mathbf{Y}_\ell^H)^{-1}\mathbf{Y}_\ell$. Then, by direct substitution of (11) and (17) in the matrix A_{ℓ} , we obtain

$$\mathbf{A}_{\ell} = \mathbf{X} \mathbf{\Gamma}_{\ell}^{1/2} \mathbf{Z}_{\ell}^{H} (\mathbf{Z}_{\ell} \mathbf{\Gamma}_{\ell} \mathbf{Z}_{\ell}^{H} + \mathbf{I})^{-1} \mathbf{Z}_{\ell} \mathbf{\Gamma}_{\ell}^{1/2} \mathbf{X}^{T} + \mathbf{U}_{\ell} (\mathbf{Z}_{\ell} \mathbf{\Gamma}_{\ell} \mathbf{Z}_{\ell}^{H} + \mathbf{I})^{-1} \mathbf{U}_{\ell}^{H} + \boldsymbol{\delta}_{\ell} + \boldsymbol{\delta}_{\ell}^{H},$$
(18)

where $\delta_\ell := \mathbf{U}_\ell (\mathbf{Z}_\ell \mathbf{\Gamma}_\ell \mathbf{Z}_\ell^H + \mathbf{I})^{-1} \mathbf{Z}_\ell \mathbf{\Gamma}_\ell^{1/2} \mathbf{X}^T$. By applying the Woodbury matrix identity on the matrix $\mathbf{C}_\ell := (\mathbf{Z}_\ell \mathbf{\Gamma}_\ell \mathbf{Z}_\ell^H +$ $\mathbf{I})^{-1}$, we get

$$\mathbf{C}_{\ell} = (\mathbf{Z}_{\ell} \mathbf{\Gamma}_{\ell} \mathbf{Z}_{\ell}^{H} + \mathbf{I})^{-1} \tag{19a}$$

$$= \mathbf{I} - \mathbf{Z}_{\ell} (\mathbf{\Gamma}_{\ell}^{-1} + \mathbf{Z}_{\ell}^{H} \mathbf{Z}_{\ell})^{-1} \mathbf{Z}_{\ell}^{H}$$
 (19b)

$$\approx \mathbf{I} - \mathbf{Z}_{\ell} (\mathbf{\Gamma_{\ell}}^{-1} + \mathbf{I})^{-1} \mathbf{Z}_{\ell}^{H} \tag{19c}$$

$$=\mathbf{I}-\mathbf{Z}_{\ell}\mathbf{D}_{\ell}\mathbf{Z}_{\ell}^{H},\tag{19d}$$

where $\mathbf{D}_{\ell} \cong \mathbf{\Gamma}_{\ell}(\mathbf{\Gamma}_{\ell} + \mathbf{I})^{-1}$. It now follows that the first term in (18) can be expressed as

$$\mathbf{T}_{\ell}^{(1)} = \mathbf{X} \mathbf{\Gamma}_{\ell}^{1/2} \mathbf{Z}_{\ell}^{H} \mathbf{C}_{\ell} \mathbf{Z}_{\ell} \mathbf{\Gamma}_{\ell}^{1/2} \mathbf{X}^{T}$$
(20a)

$$\cong \mathbf{X} \mathbf{\Gamma}_{\ell}^{1/2} (\mathbf{I} - \mathbf{D}_{\ell}) \mathbf{\Gamma}_{\ell}^{1/2} \mathbf{X}^{T}$$
(20b)

$$= \mathbf{X} \mathbf{D}_{\ell} \mathbf{X}^{T}, \tag{20c}$$

On the other hand, the second term in (18) can be written as

$$\mathbf{T}_{\ell}^{(2)} = \mathbf{U}_{\ell} \mathbf{C}_{\ell} \mathbf{U}_{\ell}^{H}$$

$$= \mathbf{U}_{\ell} \mathbf{U}_{\ell}^{H} - \mathbf{U}_{\ell} \mathbf{Z}_{\ell} \mathbf{D}_{\ell} \mathbf{Z}_{\ell}^{H} \mathbf{U}_{\ell}^{H},$$
(21a)

$$= \mathbf{U}_{\ell} \mathbf{U}_{\ell}^{H} - \mathbf{U}_{\ell} \mathbf{Z}_{\ell} \mathbf{D}_{\ell} \mathbf{Z}_{\ell}^{H} \mathbf{U}_{\ell}^{H}, \tag{21b}$$

Given that U_{ℓ} contains i.i.d entries with zero mean and variance 1/N while \mathbf{Z}_{ℓ} contains i.i.d entries with zero mean and variance $1/M_\ell$, both \mathbf{Z}_ℓ and \mathbf{U}_ℓ are uncorrelated, and $\mathbf{D}_{\ell} \preceq \mathbf{I}_{K_s}$ (\preceq interpreted element-wise), then it follows that

the summation in (21b) will be dominated by the matrix $\mathbf{U}_{\ell}\mathbf{U}_{\ell}^{H}$. Therefore, $\mathbf{T}_{\ell}^{(2)}$ can be approximately written as

$$\mathbf{T}_{\ell}^{(2)} \cong \mathbf{U}_{\ell} \mathbf{U}_{\ell}^{H}, \tag{22}$$

Then, the expression δ_{ℓ} can written as

$$\boldsymbol{\delta}_{\ell} = \mathbf{U}_{\ell} \mathbf{C}_{\ell} \mathbf{Z}_{\ell} \boldsymbol{\Gamma}_{\ell}^{1/2} \mathbf{X}^{T} \tag{23a}$$

$$\cong \mathbf{U}_{\ell} \mathbf{Z}_{\ell} (\mathbf{I} - \mathbf{D}_{\ell}) \mathbf{\Gamma}_{\ell}^{1/2} \mathbf{X}^{T}$$
(23b)

$$= \mathbf{U}_{\ell} \mathbf{Z}_{\ell} (\mathbf{\Gamma}_{\ell} + \mathbf{I})^{-1} \mathbf{\Gamma}_{\ell}^{1/2} \mathbf{X}^{T}, \tag{23c}$$

By summing (22) and (23c), we get

$$\mathbf{T}_{\ell}^{(2)} + \boldsymbol{\delta}_{\ell} = \mathbf{U}_{\ell} (\mathbf{U}_{\ell}^{H} + \mathbf{Z}_{\ell} (\boldsymbol{\Gamma}_{\ell} + \mathbf{I})^{-1} \boldsymbol{\Gamma}_{\ell}^{1/2} \mathbf{X}^{T}),$$
 (24)

where the summation on the right hand side of (24) is nothing but adding two Gaussian matrices; one with variance $\sigma_1^2 =$ 1/N and the other with variance $\sigma_2^2 = \frac{1}{N} \frac{1}{M_\ell} \sum_{i=1}^{K_s} \frac{\sqrt{\gamma_{i\ell}}}{(\gamma_{i\ell}+1)^2}$, where it can be easily seen that, even for modest M_ℓ , $\sigma_2^2 <<$ σ_1^2 . Therefore, the summation in (24) will be dominated by $\mathbf{T}_{\ell}^{(2)}$. Thus, combining (20) with (22), (18) can be written as

$$\mathbf{A}_{\ell} \cong \mathbf{X} \mathbf{D}_{\ell} \mathbf{X}^{T} + \mathbf{U}_{\ell} \mathbf{U}_{\ell}^{H}, \tag{25}$$

Recall that the optimal solution G^* of (3) is the K_c principal eigenvectors of the following matrix

$$\mathbf{A} = \sum_{\ell=1}^{L} \mathbf{A}_{\ell} \tag{26a}$$

$$= \mathbf{X}\mathbf{D}\mathbf{X}^T + \sum_{\ell=1}^{L} \mathbf{U}_{\ell}\mathbf{U}_{\ell}^H, \tag{26b}$$

where $\mathbf{D} := \sum_{\ell=1}^L \mathbf{D}_\ell \in \mathbb{R}^{K_s imes K_s}$. By defining $\mathbf{V} = [\mathbf{X}, \mathbf{U}_1, \cdots, \mathbf{U}_L] \in \mathbb{C}^{N imes (Ks + \sum_{\ell=1}^L M_\ell)}$ and $\mathbf{\Sigma} := \mathbf{V} = \mathbf{V} = \mathbf{V}$ $Diag(\mathbf{D}, \mathbf{I}_{M_1}, \cdots, \mathbf{I}_{M_L})$, (26) can be equivalently expressed

$$\mathbf{A} = \mathbf{V} \mathbf{\Sigma} \mathbf{V}^H, \tag{27}$$

Since $\mathbf{X}^T\mathbf{X} \approx \mathbf{I}_{K_s}$ and by definition $\mathbf{U}_{\ell}^H\mathbf{U}_{\ell} \approx \mathbf{I}_{M_{\ell}} \forall \ell$, then $\mathbf{V}^H\mathbf{V} \approx \mathbf{I}_{K_{\circ}+M_{\circ}}$, it can be readily seen that the right hand side of (27) is nothing but the eigendecomposition of the matrix A. Recall that the i-th diagonal entry of the matrix **D** is given by

$$\mathbf{D}_{(i,i)} = \sum_{\ell=1}^{L} r_{i\ell},\tag{28}$$

From (AS2) and by assuming that the received signal power of the k-th cell-edge user at the ℓ -th BS is few dBs above the noise floor, i.e., $r_{k\ell} > 0.5 \ \forall k = 1, \cdots, K_c$ and $\ell = 1, 2, 3$, the eigenspace of the K_c principal components of the matrix A is given by

$$\mathbf{G}^* = \mathbf{X}_c \mathbf{P},\tag{29}$$

where **P** is any $K_c \times K_c$ non-singular matrix.

REFERENCES

- E. Dahlman, S. Parkvall, and J. Skold, 4G: LTE/LTE-advanced for mobile broadband. Cambridge, MA, USA: Academic Press, 2013.
- [2] J. G. Andrews, S. Buzzi, W. Choi, S. V. Hanly, A. Lozano, A. C. Soong, and J. C. Zhang, "What will 5G be?" *IEEE J. Sel. Areas Commun.*, vol. 32, no. 6, pp. 1065–1082, June 2014.
- [3] A. J. Paulraj, D. A. Gore, R. U. Nabar, and H. Bolcskei, "An overview of MIMO communications-a key to Gigabit wireless," *Proceedings of the IEEE*, vol. 92, no. 2, pp. 198–218, Nov. 2004.
- [4] M. Jiang and L. Hanzo, "Multiuser MIMO-OFDM for next-generation wireless systems," *Proceedings of the IEEE*, vol. 95, no. 7, pp. 1430– 1469, Aug. 2007.
- [5] X. You, D. Wang, P. Zhu, and B. Sheng, "Cell edge performance of cellular mobile systems," *IEEE J. Sel. Areas Commun.*, vol. 29, no. 6, pp. 1139–1150, June 2011.
- [6] M. H. A. Khan, J.-G. Chung, and M. H. Lee, "Downlink performance of cell edge using cooperative BS for multicell cellular network," *EURASIP Journal on Wireless Communications and Networking*, vol. 2016, no. 1, p. 56, Feb. 2016.
- [7] G. Boudreau, J. Panicker, N. Guo, R. Chang, N. Wang, and S. Vrzic, "Interference coordination and cancellation for 4G networks," *IEEE Communications Magazine*, vol. 47, no. 4, Apr. 2009.
- [8] Y. Niu, Y. Li, D. Jin, L. Su, and A. V. Vasilakos, "A survey of millimeter wave communications (mmWave) for 5G: opportunities and challenges," *Wireless Networks*, vol. 21, no. 8, pp. 2657–2676, Apr. 2015.
- [9] S. Verdu et al., Multiuser detection. Cambridge, U.K.: Cambridge University Press, 1998.
- [10] H. R. Chayon, K. B. Dimyati, H. Ramiah, and A. W. Reza, "Enhanced quality of service of cell-edge user by extending modified largest weighted delay first algorithm in LTE networks," *Symmetry*, vol. 9, no. 6, p. 81, May 2017.
- [11] H. Gochev, V. Poulkov, and G. Iliev, "Improving cell edge throughput for LTE using combined uplink power control," *Telecommunication Systems*, vol. 52, no. 3, pp. 1541–1547, June 2013.
- [12] M. R. Kumar, S. Bhashyam, and D. Jalihal, "Throughput improvement for cell-edge users using selective cooperation in cellular networks," in 5th IFIP International Conference on Wireless and Optical Communications Networks, Surabaya, Indonesia, May 2008, pp. 1–5.
- [13] B. Ramamurthi, "Cutting edge at the cell edge: Co-channel interference mitigation in emerging broadband wireless systems," in First International Communication Systems and Networks and Workshops, Bangalore, India, Jan. 2009, pp. 1–7.
- [14] J. Borah, A. Hussain, and J. Bora, "Effect of intercell interference on cell boundary users in three-cell and seven-cell HetCN," *International Journal of Communication Systems*, vol. 33, no. 5, p. e4257, Nov. 2019.
- [15] R. Ghaffar and R. Knopp, "Interference suppression strategy for celledge users in the downlink," *IEEE Trans. Wireless Commun.*, vol. 11, no. 1, pp. 154–165, June 2012.
- [16] J. G. Proakis and M. Salehi, *Digital communications*. New York, NY, USA: McGraw-hill New York, 2001, vol. 4.
- [17] H. Vikalo and B. Hassibi, "The expected complexity of sphere decoding, part I: Theory, part II: Applications," *IEEE Trans. Signal Process.*, vol. 53, no. 8, p. 2819–2834, Aug. 2003.
- [18] J. Jalden and B. Ottersten, "An exponential lower bound on the expected complexity of sphere decoding," in *IEEE International Conference on Acoustics, Speech, and Signal Processing*, vol. 4, Montreal, Canada, May 2004, pp. iv–iv.
- [19] W.-K. Ma, T. N. Davidson, K. M. Wong, Z.-Q. Luo, and P.-C. Ching, "Quasi-maximum-likelihood multiuser detection using semi-definite relaxation with application to synchronous CDMA," *IEEE Trans. Signal Process.*, vol. 50, no. 4, pp. 912–922, Aug. 2002.
- [20] A. Wiesel, Y. C. Eldar, and S. Shamai, "Semidefinite relaxation for detection of 16-QAM signaling in MIMO channels," *IEEE Signal Process. Lett.*, vol. 12, no. 9, pp. 653–656, Aug. 2005.
- [21] Z.-Q. Luo, W.-K. Ma, A. M.-C. So, Y. Ye, and S. Zhang, "Semidefinite relaxation of quadratic optimization problems," *IEEE Signal Processing Magazine*, vol. 27, no. 3, pp. 20–34, May 2010.
- [22] U. Madhow and M. L. Honig, "MMSE interference suppression for direct-sequence spread-spectrum CDMA," *IEEE Trans. Commun.*, vol. 42, no. 12, pp. 3178–3188, Dec. 1994.
- [23] P. W. Wolniansky, G. J. Foschini, G. D. Golden, and R. A. Valenzuela, "V-BLAST: An architecture for realizing very high data rates over the rich-scattering wireless channel," in *International Symposium on Signals, Systems, and Electronics.*, Sept., 1998, pp. 295–300.

- [24] S. Moshavi, "Multi-user detection for DS-CDMA communications," IEEE Communications Magazine, vol. 34, no. 10, pp. 124–136, Oct. 1996.
- [25] A. Duel-Hallen, "Decorrelating decision-feedback multiuser detector for synchronous code-division multiple-access channel," *IEEE Trans. Commun.*, vol. 41, no. 2, pp. 285–290, Feb. 1993.
- [26] S. Khattak, Base Station Cooperation Strategies for Multi-user Detection in Interference Limited Cellular Systems. Dresden, Germany: Jörg Vogt Verlag, 2008.
- [27] H. Xu and P. Ren, "Joint user scheduling and power control for cell-edge performance improvement in backhaul-constrained network MIMO," in IEEE 24th Annual International Symposium on Personal, Indoor, and Mobile Radio Communications (PIMRC), London, UK, Sept. 2013, pp. 1342–1346.
- [28] C. Ubeda Castellanos, D. L. Villa, C. Rosa, K. I. Pedersen, F. D. Calabrese, P. Michaelsen, and J. Michel, "Performance of uplink fractional power control in UTRAN LTE," in *IEEE Vehicular Technology Conference (VTC)*, Singapore, May 2008, pp. 2517–2521.
- [29] S. Agarwal, S. De, S. Kumar, and H. M. Gupta, "Qos-aware downlink cooperation for cell-edge and handoff users," *IEEE Trans. Veh. Technol.*, vol. 64, no. 6, pp. 2512–2527, June 2014.
- [30] J. R. Kettenring, "Canonical analysis of several sets of variables," Biometrika, vol. 58, no. 3, pp. 433–451, 1971.
- [31] S. Khattak, W. Rave, and G. Fettweis, "Distributed iterative multiuser detection through base station cooperation," EURASIP Journal on Wireless Communications and Networking, vol. 2008, p. 17, Feb. 2008.
- [32] A. M. Rao, "Reverse link power control for managing inter-cell interference in orthogonal multiple access systems," in *IEEE 66th Vehicular Technology Conference*, MD, USA, Oct. 2007, pp. 1837–1841.
- [33] S. Das and H. Viswanathan, "Interference mitigation through intelligent scheduling," in *Proceedings of the Asilomar Conference on Signals and Systems (Asilomar)*, CA, USA, Nov. 2006.
- [34] K. Balachandran, J. H. Kang, K. Karakayali, and K. M. Rege, "Nice: A network interference cancellation engine for opportunistic uplink cooperation in wireless networks," *IEEE Trans. Wireless Commun.*, vol. 10, no. 2, pp. 540–549, Dec. 2010.
- [35] P. Marsch and G. Fettweis, "Uplink CoMP under a constrained backhaul and imperfect channel knowledge," *IEEE Trans. Wireless Commun.*, vol. 10, no. 6, pp. 1730–1742, Apr. 2011.
- [36] H. Ge, I. P. Kirsteins, and X. Wang, "Does canonical correlation analysis provide reliable information on data correlation in array processing?" in *IEEE International Conference on Acoustics, Speech and Signal Processing*, Taipei, Taiwan, May 2009, pp. 2113–2116.
- [37] Q. Wu and K. M. Wong, "Un-music and un-cle: An application of generalized correlation analysis to the estimation of the direction of arrival of signals in unknown correlated noise," *IEEE Trans. Signal Process.*, vol. 42, no. 9, pp. 2331–2343, Sept. 1994.
- [38] Z. Bai, G. Huang, and L. Yang, "A radar anti-jamming technology based on canonical correlation analysis," in *International Conference* on Neural Networks and Brain, vol. 1, Beijing, China, Oct. 2005, pp. 9–12.
- [39] Y.-O. Li, T. Adali, W. Wang, and V. D. Calhoun, "Joint blind source separation by multiset canonical correlation analysis," *IEEE Trans. Signal Process.*, vol. 57, no. 10, pp. 3918–3929, Oct. 2009.
- [40] M. Borga and H. Knutsson, "A canonical correlation approach to blind source separation," Report LiU-IMT-EX-0062 Department of Biomedical Engineering, Linkping University, 2001.
- [41] W. Liu, D. P. Mandic, and A. Cichocki, "Analysis and online realization of the CCA approach for blind source separation," *IEEE Transactions* on *Neural Networks*, vol. 18, no. 5, pp. 1505–1510, Sept. 2007.
- [42] A. Bertrand and M. Moonen, "Distributed canonical correlation analysis in wireless sensor networks with application to distributed blind source separation," *IEEE Trans. Signal Process.*, vol. 63, no. 18, pp. 4800– 4813, Sept. 2015.
- [43] R. Arora and K. Livescu, "Multi-view learning with supervision for transformed bottleneck features," in *IEEE International Conference on Acoustics, Speech and Signal Processing (ICASSP)*, Florence, Italy, May 2014, pp. 2499–2503.
- [44] J. Chen, G. Wang, and G. B. Giannakis, "Graph multiview canonical correlation analysis," *IEEE Trans. Signal Process.*, vol. 67, no. 11, pp. 2826–2838, June 2019.
- [45] M. S. Ibrahim and N. Sidiropoulos, "Cell-edge interferometry: Reliable detection of unknown cell-edge users via canonical correlation analysis," in *IEEE International Conference on Signal Processing Advances* in Wireless Communications (SPAWC), Cannes, France, July 2019, pp. 1–5.

- [46] X. Fu, K. Huang, E. E. Papalexakis, H. Song, P. P. Talukdar, N. D. Sidiropoulos, C. Faloutsos, and T. Mitchell, "Efficient and distributed algorithms for large-scale generalized canonical correlations analysis," in *IEEE 16th International Conference on Data Mining (ICDM)*, Barcelona, Spain, Dec. 2016, pp. 871–876.
- [47] X. Fu, K. Huang, M. Hong, N. D. Sidiropoulos, and A. M. So, "Scalable and flexible multiview max-var canonical correlation analysis," *IEEE Trans. Signal Process.*, vol. 65, no. 16, pp. 4150–4165, Aug. 2017.
- [48] C. I. Kanatsoulis, X. Fu, N. D. Sidiropoulos, and M. Hong, "Structured sumcor multiview canonical correlation analysis for large-scale data," *IEEE Trans. Signal Process.*, vol. 67, no. 2, pp. 306–319, Jan. 2019.
- [49] J. D. Carroll, "Generalization of canonical correlation analysis to three or more sets of variables," in *Proceedings of the 76th Annual Convention* of the American Psychological Association, vol. 3. Washington, DC, 1968, pp. 227–228.
- [50] P. Horst, "Generalized canonical correlations and their applications to experimental data," *Journal of Clinical Psychology*, vol. 17, no. 4, pp. 331–347, 1961.
- [51] A.-J. van der Veen, "Analytical method for blind binary signal separation," *IEEE Trans. Signal Process.*, vol. 45, no. 4, pp. 1078–1082, Apr. 1997.
- [52] S. Wold, K. Esbensen, and P. Geladi, "Principal component analysis," Chemometrics and Intelligent Laboratory Systems, vol. 2, no. 1-3, pp. 37–52, 1987.
- [53] D. R. Hardoon, S. Szedmak, and J. Shawe-Taylor, "Canonical correlation analysis: An overview with application to learning methods," Neural Computation, vol. 16, no. 12, pp. 2639–2664, 2004.
- [54] H. Hotelling, "Relations between two sets of variates," *Biometrika*, vol. 28, no. 3/4, pp. 321–377, Dec. 1936.
- [55] J. Rupnik, P. Skraba, J. Shawe-Taylor, and S. Guettes, "A comparison of relaxations of multiset cannonical correlation analysis and applications," arXiv preprint arXiv:1302.0974, 2013.
- [56] L.-H. Zhang, L.-Z. Liao, and L.-M. Sun, "Towards the global solution of the maximal correlation problem," *Journal of Global Optimization*, vol. 49, no. 1, pp. 91–107, Feb. 2011.
- [57] C. F. Van Loan and G. H. Golub, Matrix computations. Baltimore, MD, USA: Johns Hopkins University Press Baltimore, 1983.
- [58] M. S. Ibrahim and N. D. Sidiropoulos, "Reliable detection of unknown cell-edge users via canonical correlation analysis," *IEEE Trans. Wireless Commun.*, vol. 19, no. 6, pp. 4170–4182, Mar. 2020.
- [59] D. Gesbert, S. Hanly, H. Huang, S. S. Shitz, O. Simeone, and W. Yu, "Multi-cell MIMO cooperative networks: A new look at interference," *IEEE J. Sel. Areas Commun.*, vol. 28, no. 9, pp. 1380–1408, Oct. 2010.
- [60] R. Zhang, "Cooperative multi-cell block diagonalization with per-base-station power constraints," *IEEE J. Sel. Areas Commun.*, vol. 28, no. 9, pp. 1435–1445, Juy 2010.
- [61] M. Sorensen, C. I. Kanatsoulis, and N. D. Sidiropoulos, "Generalized canonical correlation analysis: A subspace intersection approach," *IEEE Transactions on Signal Processing*, pp. 1–1, Feb. 2021.
- [62] E. G. Larsson, O. Edfors, F. Tufvesson, and T. L. Marzetta, "Massive MIMO for next generation wireless systems," *IEEE Communications Magazine*, vol. 52, no. 2, pp. 186–195, Feb. 2014.
- [63] A. van der Veen and A. Paulraj, "An analytical constant modulus algorithm," *IEEE Transactions on Signal Processing*, vol. 44, no. 5, pp. 1136–1155, May 1996.
- [64] T. Li and N. D. Sidiropoulos, "Blind digital signal separation using successive interference cancellation iterative least squares," *IEEE Trans. Signal Process.*, vol. 48, no. 11, pp. 3146–3152, Nov. 2000.



Mohamed Salah Ibrahim (Student Member, IEEE) received the B.Sc. (with highest honors) in electrical engineering from Alexandria University, Alexandria, Egypt, in 2013, and the M.Sc. degree in wireless technologies from Nile University, Giza, Egypt, in 2016. He is currently pursuing the Ph.D. degree with the Department of Electrical and Computer Engineering, University of Virginia, Charlottesville, VA, USA. His research interests include wireless communications, signal processing, optimization, and machine learning. He was a finalist of the

Best Student Paper Competition at IEEE SPAWC 2018. He has held R&D internships at FutureWei Technologies (Huawei) in Chicago, IL, and Nokia Bell Labs in Murray Hill, NJ. He has received the Louis T. Rader Graduate Research Award from the University of Virginia, 2021.



Ahmed S. Zamzam (Member, IEEE) is a Researcher at the National Renewable Energy Laboratory, Golden, CO, where he is a member of the Power Systems Engineering Center. He obtained his PhD in Electrical Engineering from the University of Minnesota, Minneapolis, MN, in 2019. Previously, he earned his BSc at Cairo University in 2013. Ahmed received the Louis John Schnell Fellowship (2015), and the Doctoral Dissertation Fellowship (2018) from the University of Minnesota. His research interests include machine learning and

optimization of smart grids, large-scale complex energy systems, and grid data analytics.



Aritra Konar (M'17) received the B.Tech. degree in Electronics and Communications Engineering from West Bengal University of Technology, West Bengal, India, and the M.S. and Ph.D. degrees in Electrical Engineering from the University of Minnesota, Minneapolis, USA, in 2011, 2014, and 2017 respectively. He is currently a Postdoctoral Associate in the Department of ECE, University of Virginia, VA, USA. His research interests include signal processing, graph mining, nonlinear optimization and data analytics.



Nicholas D. Sidiropoulos (Fellow, IEEE) received the Diploma in electrical engineering from the Aristotle University of Thessaloniki, Thessaloniki, Greece, and the M.S. and Ph.D. degrees in electrical engineering from the University of Maryland at College Park, College Park, MD, USA, in 1988, 1990, and 1992, respectively. He has served on the faculty of the University of Virginia, the University of Minnesota, and the Technical University of Crete, Greece, prior to his current appointment as Louis T. Rader Professor and Chair of ECE at UVA. From

2015 to 2017, he was an ADC Chair Professor with the University of Minnesota. His research interests are in signal processing, communications, optimization, tensor decomposition, and factor analysis, with applications in machine learning and communications. He received the NSF/CAREER award in 1998, the IEEE Signal Processing Society (SPS) Best Paper Award in 2001, 2007, and 2011, served as IEEE SPS Distinguished Lecturer (2008–2009), and as Vice President - Membership of IEEE SPS (2017–2019). He received the 2010 IEEE Signal Processing Society Meritorious Service Award, and the 2013 Distinguished Alumni Award from the University of Maryland, Department of ECE. He is a fellow of EURASIP (2014).